Symmetrical adhesion of two cylindrical colloids to a tubular membrane*

Niu Yu-Quan(牛余全), Wei Wei(魏 巍), Zheng Bin(郑 斌), Zhang Cai-Xia(张彩霞), and Meng Qing-Tian(孟庆田)†

College of Physics and Electronics, Shandong Normal University, Jinan 250014, *China*

(Received 18 April 2013; revised manuscript received 9 July 2013)

With the full treatment of the Helfrich model we theoretically study the symmetrical adhesion of two cylindrical colloids to a tubular membrane. The adhesion of the rigid cylinders with different radius from the membrane tube surface can produce both shallow wrapping with relatively small wrapping angle and deep wrapping with big wrapping angle. These significant structural behaviors can be obtained by analyzing the system energy. A second order adhesion transition from the desorbed to weakly adhered states is found, and a first order phase transition where the cylindrical colloids undergo an abrupt transition from weakly adhered to strongly adhered states can be obtained as well.

Keywords: Helfrich model, phase transition, free energy, tubular membrane

PACS: 87.15.ad, 87.15.kt, 68.35.Np **DOI:** 10.1088/1674-1056/22/12/128701

1. Introduction

Many biological processes are controlled by the interaction of particles with cell membranes. One of the most important properties of cell membranes is their ability to control the intake of nutrients and the discharge of metabolic waste, which can make sure that the cell stays in a relatively stable internal environment.[1] The size of the particles being transported can vary from angstroms for ions such as Na^+, to micron-sized viral particles such as some animal viruses. For small particles the transport through the cell membrane is mediated by membrane proteins acting as transport channels. For micron-sized particles, however, they enter the cell by endocytosis and exit the cell by exocytosis.[2,3] During both processes the membrane envelops the particles that deform the membrane on a scale much larger than its thickness.

In order to simulate the wrapping and budding processes in cells and interactions between particles mediated by a fluid membrane, a number of models with related parameters for the adhesion of particles to interfaces of membranes were designed and theoretically studied.[4–12] By treating the nonlinearity in bending elasticity through the Bogomol'nyi decomposition technique and elastic compatibility, Jérôme Benoit and Avadh Saxena[13] solved the problem of the global shape description of a spherical vesicle distorted by a grafted latex bead. Deserno and coworkers[14–16] examined the elastic deformation of a fluid membrane induced by adhering spherical colloidal particles within the framework of the Helfrich energy model;[4–8] structural and energetic aspects were discussed in detail. Both continuous binding and discontinuous envelopment transitions were observed for spherical particles. Recently Chen *et al.*[17–22] and other researchers[23–25] have made theoretical efforts to examine the structure and transport properties in systems involving tubular membranes or rigid particles, such as a single or multiple spherical particles adhered to the interior of a membrane tube, or the systems of a confined polymer inside a soft tube and the adhesion of a cylinder to a soft tube. Sergey *et al.*[21] also investigated one and two cylinders adhered to a membrane surface in different ways. The analysis of the free energy leads to the conclusion that different phase transitions exist in these simple systems.

As an idealized model, the cylindrical particle-membrane tube system has been widely used to provide fundamental understanding of the physical properties of biological systems. For example, a cylindrical particle can represent MVL51 rod phage.[26] On special occasions this model can also provide profound structural properties for any baculovirus interacting with a columnar cell.

The present work intends to examine the system of two rigid cylindrical particles interacting with a soft tube symmetrically, where the radius of the tube wall is larger than that of the rigid cylindrical particle. This elementary yet meaningful model is applicable to soft matter research and other numerous phenomena in natural and living systems related to rod phages or baculovirus. The successful utilization of a similar model in describing particle-membrane adhering systems can be exemplified by a cylindrical colloid adsorbed on tubular membranes investigated by Chen *et al.*,[22] hereafter we shall refer to this system as the one-cylinder system. In the next section we will derive the expression of the free energy based on the Helfrich model, and obtain the shape function of the membrane pro-

*Project supported by the National Natural Science Foundation of China (Grant No. 11074151) and the National Key Basic Research and Development Program of China (Grant No. 2011CB808100).

†Corresponding author. E-mail: qtmeng@sdnu.edu.cn

© 2013 Chinese Physical Society and IOP Publishing Ltd

file by solving the Hamilton canonical equations. From the numerical search for the minimum of the total free energy we can determine the stability structure of the system in Section 3. Also discussed in this section is the process of phase transition involving three phases consisting of desorption, shallow wrapping adhesion, and deep wrapping adhesion. Finally in Section 4, we summarize our main conclusions.

2. Free energy model

Consider a system that two cylindrical particles adhere to a soft tube membrane symmetrically. When the tube is much longer than the rigid cylindrical particle, the variation of the membrane shape in the direction parallel to the tube itself can be completely ignored, and the much smaller radius of the rigid cylindrical particle than the tube radius will enable us to describe the biology phenomena more accurately. If the membrane shape is represented by a curve, which undergoes a radial change in the process of membrane deforming, the system can be reduced to a two-dimensional model. From the cross section view (Fig. 1), we can see that this system is further represented by two rigid circles interacting with a deformable closed curve. In this case, the membrane shape can then be described by the tangent angle $\psi(s)$ and the coordinate circle radius $r(s)$. Both of them are the functions of the contour variable s, with $\psi(s)$ being with respect to the coordinate circle of $r(s)$, γ being the wrapping angle and α, θ being also defined in the cross section view. Every point in the membrane is subject to such constraints as

$$\frac{\mathrm{d}r}{\mathrm{d}s} = \sin\psi(s), \tag{1}$$

$$r(s)\frac{\mathrm{d}\theta}{\mathrm{d}s} = \cos\psi(s), \tag{2}$$

and the bending curvature of the membrane at s can be written as

$$\frac{\mathrm{d}(\theta-\psi)}{\mathrm{d}s}. \tag{3}$$

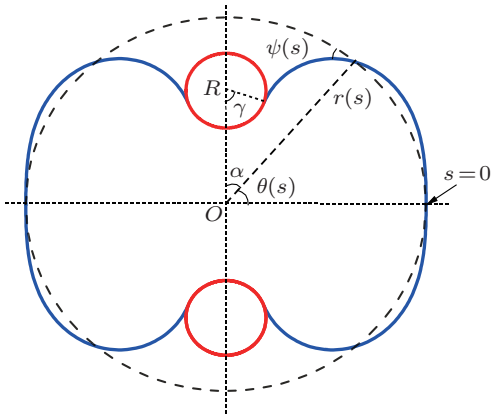


Fig. 1. (color online) Cross section sketch of the adhesion of two rigid cylindrical particles (red) with radius R to the exterior surface of a soft membrane tube (blue) that is originally a circular cylinder with radius r_0, which is perpendicular to the cylinder axis.

In this paper, the energy of the two-dimensional elastic tube is considered to follow the Helfrich model for a fluid membrane, which contains two parameters, i.e., bending rigidity κ and surface tension σ. We assume that a short-range attraction exists between the surfaces of the membrane tube and the rigid cylindrical particles, which can be effectively represented by w, the adhesion energy of the unit area. So the energy of the membrane tube adsorbed to the cylinders can be described by three energy contributions: adhesion energy, bending energy, and tension energy of the membrane, which are represented by w, κ, and σ, respectively.

The total free energy of the system is composed from the energy of the free part membrane and the one corresponding to the membrane which is adhered on the cylinder. Relative to finding the energy for the adhered part, giving the energy for the free part of the membrane is an involved work because this energy is the function of the membrane shape and needs to be minimized with respect to it first. Suppose the length of the deformed membrane tube is L, the free energy of the non-adhering portion can then be written as

$$E_{\mathrm{free}} = 4L\int_0^S \mathrm{d}s\left[\frac{\kappa}{2}\left(\frac{\mathrm{d}(\theta-\psi)}{\mathrm{d}s}\right)^2+\sigma\right], \tag{4}$$

where the path variable s goes from $s=0$ to $s=S$, and S is the curve length up to the contact point. With the constrain (2) the free energy can also be written as

$$E_{\mathrm{free}} = 4L\int_0^S \mathrm{d}s\left[\frac{\kappa}{2}\left(\frac{\cos\psi}{r}-\frac{\mathrm{d}\psi}{\mathrm{d}s}\right)^2+\sigma\right]. \tag{5}$$

Note that a prefactor of 4 has been included to account for four quarters of the non-adhering parts of the membrane.

For a free membrane tube with no cylindrical colloid adhesion, $\psi(s)=0$, $r_0=r(s)=2S/\pi$, and $\theta(s)=s\pi/2S$. From the minimization of its free energy

$$E_{\mathrm{free}} = 4LS\left(\frac{\kappa}{2r_0^2}+\sigma\right), \tag{6}$$

we obtain a uniform square radius

$$r_0^2 = \frac{\kappa}{2\sigma}. \tag{7}$$

Using r_0 as the basic length scale, it is convenient to introduce the following dimensionless quantities $\tilde{s}=s/r_0$, $\tilde{r}=r/r_0$, consequently, the constraints of Eqs. (1) and (2) can be written as

$$\frac{\mathrm{d}\tilde{r}}{\mathrm{d}\tilde{s}} = \sin\psi, \tag{8}$$

$$\frac{\mathrm{d}\theta}{\mathrm{d}\tilde{s}} = \frac{\cos\psi}{\tilde{r}}, \tag{9}$$

so the reduced energy have the following form

$$\tilde{E}_{\mathrm{free}} = \frac{E_{\mathrm{free}}r_0}{4\kappa L} = \frac{1}{2}\int_0^{\tilde{S}}\mathrm{d}\tilde{s}\left[\left(\frac{\cos\psi}{\tilde{r}}-\frac{d\psi}{d\tilde{s}}\right)^2+1\right]. \tag{10}$$

For the original circular tube of radius r_0, the free energy from the current model has the form

$$E_0 = 4L\int_0^S \mathrm{d}s\left[\frac{\kappa}{2}\left(\frac{\mathrm{d}\theta}{\mathrm{d}s}\right)^2+\sigma\right], \tag{11}$$

and the correspondent reduced energy is

$$\tilde{E}_0 = \int_0^{\tilde{S}} \mathrm{d}\tilde{s}\frac{\mathrm{d}\theta}{\mathrm{d}\tilde{s}} = \int_0^{\tilde{S}} \mathrm{d}\tilde{s}\frac{\cos\psi}{\tilde{r}}. \tag{12}$$

With reference to the free energy of a freely standing, the reduced free energy difference for the non-adhering portion of the membrane can be expressed as

$$\begin{aligned}\tilde{E}_{\mathrm{free}}-\tilde{E}_0 &= \Delta\tilde{E}_{\mathrm{free}}\\ &= \int_0^{\tilde{S}} \mathrm{d}\tilde{s}\left[\frac{1}{2}\left(\frac{\cos\psi}{\tilde{r}}-\frac{\mathrm{d}\psi}{\mathrm{d}\tilde{s}}\right)^2+\frac{1}{2}-\frac{\cos\psi}{\tilde{r}}\right].\end{aligned} \tag{13}$$

At the given wrapping angle γ, the shape function of the tube, $\psi(s)$, is determined by minimizing the above integral term together with the additional term that includes the constraints (8) and (9). To do so, we introduce the Hamilton canonical equation and write the effective Lagrangian function as

$$\begin{aligned}L &= \frac{1}{2}\left(\frac{\cos\psi}{\tilde{r}}-\dot{\psi}\right)^2+\frac{1}{2}-\frac{\cos\psi}{\tilde{r}}\\ &\quad+\lambda(\tilde{s})[\dot{\tilde{r}}-\sin\psi(\tilde{s})],\end{aligned} \tag{14}$$

where $\lambda(\tilde{s})$ is a Lagrangian multiplier function. Then the canonical momenta P_ψ and P_r have the forms

$$P_\psi(\tilde{s}) = \frac{\partial L}{\partial\dot{\psi}} = \dot{\psi}-\frac{\cos\psi}{\tilde{r}}, \tag{15}$$

$$P_r(\tilde{s}) = \frac{\partial L}{\partial\dot{\tilde{r}}} = \lambda(\tilde{s}), \tag{16}$$

respectively, and the total Hamiltonian function H assumes the form

$$\begin{aligned}H &= P_\psi\dot{\psi}+P_r\dot{r}-L = \frac{P_\psi^2}{2}+\frac{P_\psi\cos\psi}{\tilde{r}}\\ &\quad+\frac{\cos\psi}{\tilde{r}}-\frac{1}{2}+P_r\sin\psi,\end{aligned} \tag{17}$$

where the dot indicates a derivative with respect to the arc length $\tilde{s}$.

Using the treatment of the canonical equations of motion in Hamiltonian dynamics, the minimization of the free energy difference comes down to solving four coupled differential equations for four functions $\psi(\tilde{s})$, $P_\psi(\tilde{s})$, $P_r(\tilde{s})$, and $\tilde{r}(\tilde{s})$

$$\frac{\mathrm{d}\psi}{\mathrm{d}\tilde{s}} = P_\psi+\frac{\cos\psi}{\tilde{r}}, \tag{18}$$

$$\frac{\mathrm{d}P_\psi}{\mathrm{d}\tilde{s}} = (P_\psi+1)\frac{\sin\psi}{\tilde{r}}-P_r\cos\psi, \tag{19}$$

$$\frac{\mathrm{d}P_r}{\mathrm{d}\tilde{s}} = \frac{(P_\psi+1)\cos\psi}{\tilde{r}^2}, \tag{20}$$

$$\frac{\mathrm{d}\tilde{r}}{\mathrm{d}\tilde{s}} = \sin\psi, \tag{21}$$

with the boundary conditions

$$\psi(0)=0,\quad P_\psi(0)=\xi,\quad P_r(0)=\zeta,\quad \tilde{r}(0)=1, \tag{22}$$

at the start point $\tilde{s}=0$. Here ξ and ζ are two unknown free parameters to be determined below. At the endpoint $\tilde{s}=\tilde{S}$, the membrane curve tangentially adheres to the surface of the rigid cylinders, which further produces two connection conditions involving the reduced cylinder radius $\tilde{R}$ and wrapping angle γ at $\tilde{s}=\tilde{S}$

$$\gamma = \theta(\tilde{S})-\psi(\tilde{S})-\frac{\pi}{2}, \tag{23}$$

$$\tilde{R} = \frac{\tilde{r}(\tilde{S})\cos\theta(\tilde{S})}{\sin\gamma}, \tag{24}$$

where $\theta(s)$ is the angle between $r(0)$ and $r(s)$, and can be obtained from Eq. (9).

To solve the first-order differential Eqs. (18)–(21) numerically, as usual, we use the shooting method to integrate these equations from $\tilde{s}=0$ to $\tilde{s}=\tilde{S}$ with conditions (22) and the pre-set ξ and ζ until the targeted boundary conditions (23) and (24) are numerically satisfied. The numerical procedure yields the shape function $\psi(s)$ and the corresponding free energy for the given γ. Obviously the free energy is the function of wrapping angle γ.

Assuming that the adhering membrane remains in the fluid state, for the adhered part of the membrane, the shape is that of the cylinder it adheres to. Once the degree of wrapping angle γ is known, the corresponding reduced energy difference can be easily calculated as

$$\Delta\tilde{E}_{\mathrm{contact}} = \tilde{w}\gamma\tilde{R}+\frac{\gamma}{2\tilde{R}}+\frac{\gamma\tilde{R}}{2}-\alpha, \tag{25}$$

where $\tilde{w}=wr_0^2/\kappa$ denotes the reduced adhesion energy. Together with Eq. (13), we obtain the total reduced free energy difference of the system

$$\Delta\tilde{E} = \Delta\tilde{E}_{\mathrm{free}}+\Delta\tilde{E}_{\mathrm{contact}}, \tag{26}$$

where $\Delta\tilde{E}_{\mathrm{free}}$ describes the free energy difference of the free part of the membrane. For the entire system the task then becomes to minimize the total energy for determination of the stable structure.

3. Results and discussion

3.1. Equilibrium profile

Now we first discuss the process of two rigid cylinders adhering to a membrane tube symmetrically. At a smaller adhesion energy $|\tilde{w}|$, the rigid cylinders and the membrane keep a free or desorption state, and the membrane shape remains almost a perfect circle and the area inside is not changed without the contact area (the black solid curves in Fig. 2 (labeled as

a). With increasing of the adhesion energy $|\tilde{w}|$, the desorption state translates to the shallow wrapping, where the membrane shape presents a slight distortion (the red short dotted curves in Fig. 2 (labeled as *b*). As $|\tilde{w}|$ increases further, the equilibrium profile is of the deep wrapping state or the full envelopment wrapping, where the membrane wraps two cylinders completely (the blue dashed curve in Fig. 2 (labeled as *c*).

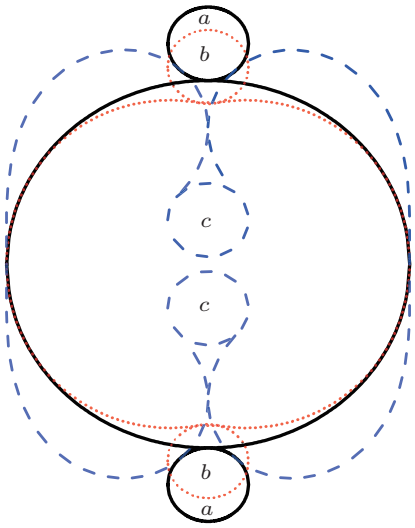


Fig. 2. (color online) The process of the second order phase transition from desorption (*a*) (the black solid curve) to shallow wrapping (*b*) (the red short dotted curve), and the process of the first order phase transition from shallow wrapping (*b*) to deep wrapping (*c*) (the blue dashed curve) for two cylinders adhering to the membrane tube.

The transition from free to shallow wrapping can be seen from the changing of Fig. 2 (*a*) to Fig. 2 (*b*), where the membrane cross section produces a little deformation but the entire conformation remains approximately circular. However, in the transition from shallow wrapping to full envelopment wrapping as given by the changing of Fig. 2 (*b*) to Fig. 2 (*c*), the wrapping angle γ and the distance between rigid cylinders make a jump, and the major portion of the cylinder is in contact with the membrane. In this case because of the full wrapping of the two cylinders, the equilibrium shape profiles of the membrane are different from the previous results. In the following sections these different transitions will be called the second and first order phase transitions, respectively.

The variation of wrapping angle γ as a function of $|\tilde{w}|$ around the transition points is illustrated in Fig. 3. It is clear that at around $|\tilde{w}| = 589.3$, 220.5, 60.5, and 18.5 for $\tilde{R} = 0.03$, 0.05, 0.10, and 0.20, respectively, the change of γ is continuous. Since we know that for the membrane system without adhesion, the membrane will keep its original shape, we can easily deduce that for the system of given $\tilde{R}$, when $|\tilde{w}|$ is relatively smaller, the membrane free energy without the contribution of adhesion energy dominates the total system, and hence the shallow wrapping shapes are more stable. Comparing with the one-cylinder system, the wrapping angle transition point is similar and γ is approximately equal to 0.2. At around $|\tilde{w}| = 606.3$, 230.7, 65.8, and 23.5 for $\tilde{R} = 0.03$, 0.05, 0.10, and 0.20, respectively, however, the change of γ is discontinuous (Fig. 3). For a given $\tilde{R}$, when $|\tilde{w}|$ is relatively larger, the adhesion energy prefers a more complete wrapping of membrane on the two cylinders.

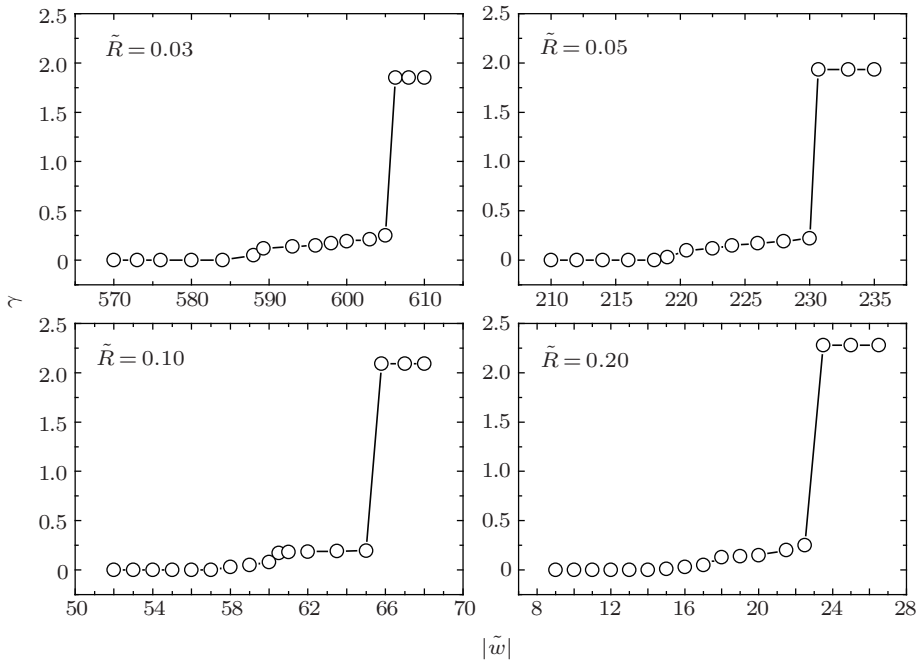


Fig. 3. Wrapping angle γ as functions of unit area adhesion energy $|\tilde{w}|$ corresponding to the free energy minimum for selected values of reduced radius $\tilde{R}$.

As discussed above, the membrane shape is the function of total reduced free energy. With the extension of the wrapping part, the increased adhesion energy will change the total reduced free energy, and the minimization of the free energy gives rise to the stable membrane shape. In our calculation, one of the considered states is the deep wrapping state before the membrane just contacts itself, the limit of which can be represented by the abscissa value of the free point on the membrane being zero, i.e., the point contact of the membrane itself, and the surface contact of the membrane is beyond our discussion. Certainly the two contact points are symmetrical with reference to the horizontal (see Fig. 2 (*c*)). From the comparison between our calculation and the work for the one-cylinder system, we can find that when $\tilde{R} \leq 0.1$ the wrapping angle transition point is similar, but when $\tilde{R} > 0.1$, it has a larger value in our work. The conformation of system changing with radius $\tilde{R}$ at shallow wrapping and deep wrapping states can be also depicted vividly in Fig. 4(a) and 4(b), respectively. At the deep wrapping states shown in Fig. 4(b), the distance between the cylinders increases gradually in the region of $\tilde{R} \leq 0.1$, while in the region of $\tilde{R} > 0.1$, it has a contrary tendency. The minimum distance of the membrane on both sides of the cylinder has somewhat different characteristics with the one-cylinder system. In the region of $\tilde{R} < 0.05$, the membrane touches itself on the top of the cylinder, and when $\tilde{R} = 0.05$ the two wings of membrane separate from each other. With increasing of $\tilde{R}$, this distance decreases further, and the membrane touches itself again.

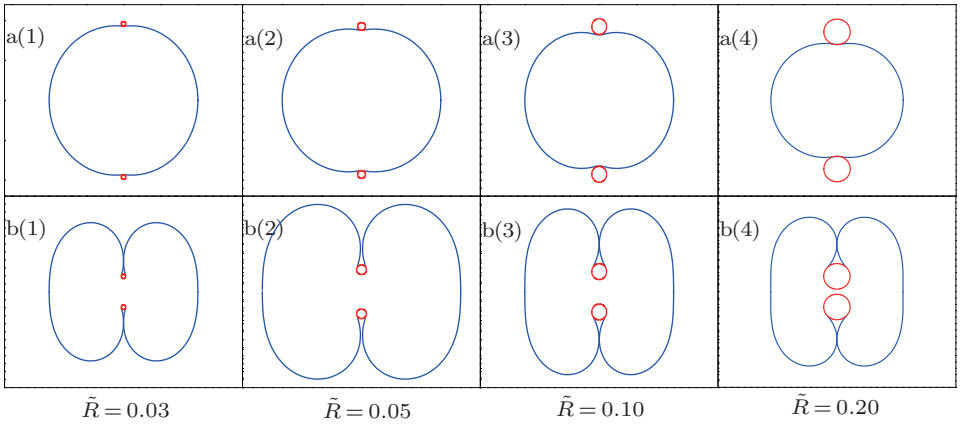


Fig. 4. (color online) Cross section profiles of the tubular membrane (blue) at the shallow wrapping states (a(1)–a(4)), and the deep wrapping states (b(1)–b(4)), for $\tilde{R} = 0.03$, 0.05, 0.10, and 0.20, respectively.

3.2. Phase transition

Both Fig. 3 and Fig. 4 have already shown us obviously that the relative position of the cylinder and membrane (or adhesion property) has to do with reduced radius $\tilde{R}$ and adhesion energy $|\tilde{w}|$. In fact this changing characteristic can also be presented by the so-called phase diagram drawn in a parameter space spanned by the reduced adhesion energy $|\tilde{w}|$ and radius ratio $\tilde{R}$. When the wrapping angle γ varies continuously with the increase of $|\tilde{w}|$, this phase transition is referred to the second order phase transition. On the contrary, when the wrapping angle γ has a jump with the increase of $|\tilde{w}|$, this transition is referred to the first order phase transition.[27,28]

3.2.1. The second order phase transition

For the fixed reduced radius $\tilde{R}$, the characteristic of this phase transition is the wrapping angle γ, which can be determined by a numerical analysis. Looping through the table of the free energy difference coming from the numerical procedure, we can find the free energy minimum as a function of γ at the given $|\tilde{w}|$. When $|\tilde{w}|$ is smaller, the free energy difference minimum only has a zero value with the wrapping angle $\gamma_0 = 0$, and the system is in a desorption state. With the increase of adhesion energy $|\tilde{w}|$, the system reaches the transition point where $|\tilde{w}| = |\tilde{w}_0|$, and the free energy difference minimum becomes weakly negative with the small wrapping angle γ. Both the $|\tilde{w}_0|$ and the corresponding $\tilde{R}$ represent a critical point at the second order transition boundary.

Take $\tilde{R} = 0.10$ as an example, where a second order transition takes place at $|\tilde{w}| = 60.5$. We have plotted in Fig. 5 the free energy difference as a function of the wrapping angle γ to demonstrate the second order transition. Obviously there is a free energy difference minimum at the wrapping angle $\gamma \approx 0.17$. Both $\tilde{R} = 0.10$ and $|\tilde{w}_0| = 60.5$ represent a critical point at the second order transition boundary as shown in Fig. 6 (red circles). In this figure, the whole region is divided into three regions, i.e., desorption state (region I), shallow wrapping state (region II), and deep wrapping state (region III). At given $|\tilde{w}_0| = 60.5$, when $\tilde{R} < 0.10$, the points are in region I, and when $0.10 < \tilde{R} < 0.11$, the points are in region II.

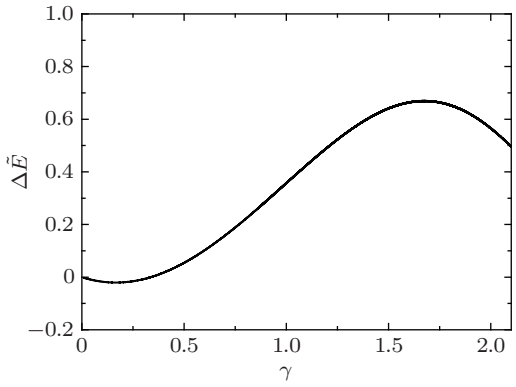


Fig. 5. The reduced free energy difference $\Delta\tilde{E}$ depending on the wrapping angle γ for reduced radius $\tilde{R}$=0.10 at the second order transition when the adhesion energy $|\tilde{w}|$ reaches 60.5.

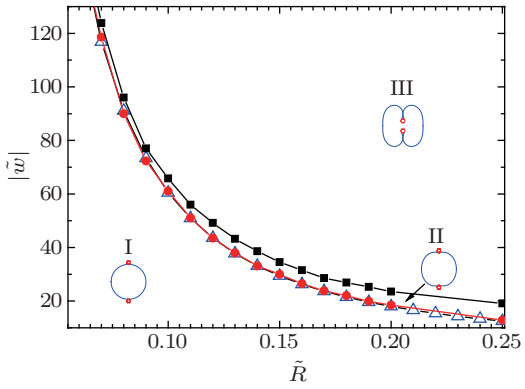


Fig. 6. (color online) Phase diagram for the adhesion of two rigid cylinders of radius R to an originally cylindrical membrane tube of radius r_0, in a parameter space spanned by the reduced adhesion energy $|\tilde{w}|$ and radius ratio $\tilde{R}$. The curve associated with red circles symbols is a second order phase boundary between the desorption (region I) and shallow wrapping states (region II). Black squares represent our numerical results for the first order phase boundary between the shallow wrapping (region II) and deep wrapping state (region III). Blue triangles represent the analytic results for the second order phase boundary.

The second order phase transition can also be independently determined on the basis of small angle expansion. Corresponding to a weakly deformed membrane shape $\psi \approx 0$ and $\tilde{r}_0 \approx 1$, keeping the term of linear order in ψ and dropping all higher order terms from Eq. (13), we have

$$\Delta\tilde{E}_{\text{free}} = \int_0^{\tilde{S}} \mathrm{d}\tilde{s} \left[\frac{1}{2}\left(\frac{\mathrm{d}\psi}{\mathrm{d}\tilde{s}}\right)^2 - \frac{\cos\psi}{\tilde{r}}\frac{\mathrm{d}\psi}{\mathrm{d}\tilde{s}} + \frac{1}{2}\left(\frac{\cos\psi}{\tilde{r}} - 1\right)^2 \right]$$
$$= \int_0^{\tilde{S}} \mathrm{d}\tilde{s} \left(-\frac{\mathrm{d}\psi}{\mathrm{d}\tilde{s}} \right) = -\psi(\tilde{S}). \tag{27}$$

Combining with the geometrical relationship $\alpha = -\gamma - \psi(\tilde{S})$, with the reduced adhesion energy $\tilde{w} = wr_0^2/\kappa$ the total reduced free energy difference of the system can be written as

$$\Delta\tilde{E} = \left[\left(\frac{1}{2\tilde{R}^2} + \frac{1}{2} + \tilde{w} \right) \tilde{R} + 1 \right] \gamma. \tag{28}$$

Then the critical point is determined by the requirement that the coefficient of the γ term vanishes, which yields

$$\tilde{w} = -\left(\frac{1}{2} + \frac{1}{\tilde{R}} + \frac{1}{2\tilde{R}^2} \right). \tag{29}$$

According to Eq. (29), we can obtain the relationship of $|\tilde{w}|$ and $\tilde{R}$ drawn in Fig. 6 as the solid curve by blue triangles. Obviously the changing tendency obtained from the analytic result agrees with the numerical result excellently.

3.2.2. The first order phase transition

Relative to the second order phase transition, which corresponds to the continuous change of wrapping angle γ with increasing of $|\tilde{w}|$, the first order phase transition is characterized by the discontinuity of wrapping angle γ by varying $|\tilde{w}|$ across the phase boundary (Fig. 3). The existence of shallow and deep adhesions was also observed in related membrane systems described by the same energy model.[19,20] For the given value of $\tilde{R}$ by gradually increasing the adhesion energy $|\tilde{w}|$, we can find two almost equal minimum energy differences as $|\tilde{w}|$ approaches to the second transition point $|\tilde{w}_1|$. Both $|\tilde{w}_1|$ and the corresponding $\tilde{R}$ represent a critical point at the first order transition boundary. For different reduced radius $\tilde{R}$, the similar manner as above can give a series of $|\tilde{w}_1|$, by which one can draw a phase boundary curve as shown in Fig. 6 by black squares. Obviously, at given $|\tilde{w}_0| = 60.5$, when $\tilde{R} > 0.11$, the points are in region III.

A typical wrapping angle and energy relation curve for $\tilde{R} = 0.10$ at the wrapping transition point $|\tilde{w}_1|$ is shown in Fig. 7. At this point, there exist two approximately equal energy minima which correspond to $\gamma = 0.37$ and $\gamma = 2.09$, respectively. At the small wrapping angle $\gamma = 0.37$, the stable state is of shallow wrapping. As the wrapping angle increases, the energy ascends to reach an energy maximum and then descends to a second energy minimum with the wrapping angle $\gamma = 2.09$. At this large wrapping angle, the stable state is of deep wrapping. The energy barrier separates the wrapping state into the fully and partially wrapped states as shown in Fig. 7, which renders the transition discontinuous.

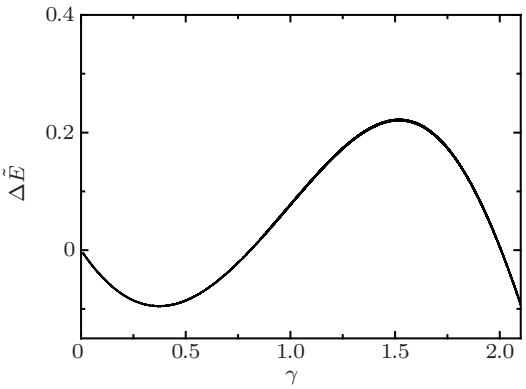


Fig. 7. The reduced free energy difference $\Delta\tilde{E}$ depending on the wrapping angle γ for the reduced radius $\tilde{R} = 0.10$ at the first order transition when the adhesion energy $|\tilde{w}|$ reach to 65.8.

As we know, many phase boundaries are heavily influenced by the presence of the excluded volume conditions between the cylinder particles and membrane tube, as well as

between two separate portions of membrane tube. This is the reason why when the wrapping angle γ is larger than 2.09, the obtained $\Delta\tilde{E} - \gamma$ curve is not reasonably continuous, which implies, in particular, that the membrane tube curve cannot intersect the cylinder particles at the adhering portion. Just for this reason, in our calculation the numerical solutions which violate these conditions have been ruled out.

In addition, we notice that for the one-cylinder system,[22] a similar phase diagram to us (Fig. 6) was given, in which the transition from desorption to partial wrapping phases was shown to be a second order transition, and the transition from the partial wrapping to enveloped states was shown to be the first order one. However in our calculation, because of the limitation of the shooting method used, the target is too sensitive to the initial selection of ξ and ζ, it is difficult for us to find the first order phase transition for the $\tilde{R}$ larger than 0.25.

4. Summary

Within the framework of the Helfrich energy model, we have systematically investigated the shapes of a membrane tube symmetrically adhering to two cylindrical colloids. Based on a full optimization of the membrane shape, the free energy difference of the system is given, and the total free energy difference of the system is then analyzed for the phase behavior. Starting from the simple energy model, it is demonstrated that there exists a phase diagram as two rigid cylinder particles adhere to a membrane tube. Continuous and discontinuous envelopment transitions represent, respectively, the desorbed to weakly adhered state and the weakly adhered to deeply adhered state, and the latter displays a potentially substantial energy barrier. The calculated phase diagram provides a basis for understanding the structural transformations in practical systems, such as virus-vesicle endocytosis and nanoparticle vesicle complexes. We also find the interaction of the rigid cylinder with different radius from the deformed surface of the membrane tube can produce two main states: weakly adhered and strongly adhered states. It remains theoretically and numerically challenging to treat asymmetric conformations, which may include more plentiful possible results.

Acknowledgments

The authors thank Jeff Z. Y. Chen from University of Waterloo for his technical support, instructive advice, and useful suggestions.

References

[1] Lodish H, Berk A, Zipursky S L, Matsudaira P, Baltimore D and Darnell J 2000 *Molecular Cell Biology* (New York: W. H. Freeman and Company)
[2] Pietiainen V, Marjomaki V, Upla P, Pelkmans L, Helenius A and Hyypia T 2004 *Mol. Biol. Cell* **15** 4911
[3] Sieczkarski S B and Whittaker G R 2002 *J. Gen. Virol.* **83** 1535
[4] Helfrich W, Servuss R M and Undulations 1984 *Nuovo Cimento D* **3** 137
[5] Helfrich W 1973 *Z. Naturforsch C* **28** 693
[6] Ouyang Z C and Helfrich W 1987 *Phys. Rev. Lett.* **59** 2486
[7] Ouyang Z C and Helfrich W 1989 *Phys. Rev. A* **39** 5280
[8] Tu Z C and Ouyang Z C 2003 *Phys. Rev. E* **68** 061915
[9] Tu Z C 2013 *Chin. Phys. B* **22** 028701
[10] Peng Y G and Zheng Y J 2011 *Acta Phys. Sin.* **60** 088701 (in Chinese)
[11] Smith A S, Sackmann E and Seifert U 2004 *Phys. Rev. Lett.* **92** 208101
[12] Tsafrir I, Sagi D, Arzi T, Frette V, Kandel D and Stavans J 2001 *Phys. Rev. Lett.* **86** 1138
[13] Benoit J and Saxena A 2007 *Phys. Rev. E* **76** 041912
[14] Deserno M 2004 *Phys. Rev. E* **69** 031903
[15] Müller M M and Deserno M 2007 *Phys. Rev. E* **76** 011921
[16] Deserno M and Gelbart W M 2002 *J. Phys. Chem. B* **106** 5543
[17] Chen Jeff Z Y 2010 *Phys. Rev. E* **82** 060801
[18] Chen Jeff Z Y 2007 *Phys. Rev. Lett.* **98** 088302
[19] Chen Jeff Z Y, Liu Y and Liang H J 2009 *Phys. Rev. Lett.* **102** 168103
[20] Cao S Q, Wei G H and Chen Jeff Z Y 2011 *Phys. Rev. E* **84** 050901
[21] Mkrtchyan S, Ing C and Chen Jeff Z Y 2010 *Phys. Rev. E* **81** 011904
[22] Chen Jeff Z Y and Mkrtchyan S 2010 *Phys. Rev. E* **81** 041906
[23] Derenyi I, Julicher F and Prost J 2002 *Phys. Rev. Lett.* **88** 238101
[24] Roux A, Cappello G, Cartaud J, Prost J, Goud B and Bassereau P 2002 *Proc. Natl. Acad. Sci. USA* **99** 5394
[25] Tsafrir I, Caspi Y, Guedeau-Boudeville M A, Arzi T and Stavans J 2003 *Phys. Rev. Lett.* **91** 138102
[26] Das J and Jack M 1976 *Proc. Natl. Acad. Sci. USA* **73** 1489
[27] Paczuski M and Kardar M 1988 *Phys. Rev. Lett.* **60** 2638
[28] Koibuchi H and Kuwahata T 2005 *Phys. Rev. E* **72** 026124